Central and Peripheral Changes in Retinal Vein Occlusion and Fellow Eyes in Ultra-Widefield Optical Coherence Tomography Angiography

Xin-yu Zhao,[1,2] Qing Zhao,[1,2] Chu-ting Wang,[1,2] Li-hui Meng,[1,2] Shi-yu Cheng,[1,2] Xing-wang Gu,[1,2] Srinivas R. Sadda,[3,4] and You-xin Chen[1,2]

[1]Department of Ophthalmology, Peking Union Medical College Hospital, Chinese Academy of Medical Sciences, Beijing, China
[2]Key Laboratory of Ocular Fundus Diseases, Chinese Academy of Medical Sciences & Peking Union Medical College, Beijing, China
[3]Doheny Eye Institute, Pasadena, California, United States
[4]Department of Ophthalmology, David Geffen School of Medicine, University of California, Los Angeles, Los Angeles, California, United States

Correspondence: You-xin Chen, Department of Ophthalmology, Peking Union Medical College Hospital, Chinese Academy of Medical Sciences, No.1 Shuaifuyuan, Wangfujing, Dongcheng District, Beijing 100730, China; chenyx@pumch.cn.
Srinivas R. Sadda, Department of Ophthalmology, Doheny Eye Institute, 1355 San Pablo Street, Suite 211, Los Angeles, CA 90033, USA; ssadda@doheny.org.

XZ and QZ contributed equally to the work presented here and should therefore be regarded as equivalent authors.

Received: July 30, 2023
Accepted: December 26, 2023
Published: February 2, 2024

Citation: Zhao X, Zhao Q, Wang C, et al. Central and peripheral changes in retinal vein occlusion and fellow eyes in ultra-widefield optical coherence tomography angiography. *Invest Ophthalmol Vis Sci.* 2024;65(2):6. https://doi.org/10.1167/iovs.65.2.6

Purpose. To explore the central and peripheral retinal and choroidal changes in retinal vein occlusion (RVO) and fellow eyes using ultra-widefield swept-source optical coherence tomography angiography (UWF-SS-OCTA).

Methods. Fifteen ischemic central RVO (CRVO), 15 branch RVO (BRVO), and 15 age-matched healthy controls were prospectively recruited. Retinal and choroidal parameters, including retinal vessel flow density (VFD) and vessel linear density (VLD), choroidal vascularity volume (CVV), choroidal vascularity index (CVI), and VFD in the large and medium choroidal vessels (LMCV-VFD), were measured in the central and peripheral regions of the 24 × 20-mm UWF-SS-OCTA images.

Results. Ischemic CRVO and BRVO eyes showed increased foveal avascular zone area, perimeter, and acircularity index (AI) compared to their fellow eyes and healthy control eyes, and RVO fellow eyes also had larger AI values than controls ($P < 0.05$). For ischemic CRVO and BRVO eyes versus control eyes, VFD, VLD, CVV, CVI, and LMCV-VFD decreased, but retinal thickness and volume in the superficial capillary plexus, deep capillary plexus, and whole retina increased ($P < 0.05$). Moreover, RVO fellow eyes also showed significantly decreased retinal VFD, LMCV-VFD, and CVI, as well as increased retinal thickness and volume, compared with control eyes ($P < 0.05$). Alterations were not consistent throughout the retina, as they involved only the peripheral or central regions in some cases.

Conclusions. The affected and unaffected fellow eyes of RVO patients both demonstrated central and/or peripheral structural and vascular alterations in the retina and choroid. Because UWF-SS-OCTA enables visualization and evaluation of the vasculature outside the posterior pole, it presents a promising approach to more fully characterize vascular alterations in RVO.

Keywords: ultra-widefield optical coherence tomography angiography, retinal vein occlusion, retina, choroid

Retinal vein occlusion (RVO) is one of the most common retinal vasculopathies, with a global prevalence of 0.77% among people 30 to 89 years of age, which is equivalent to 28.06 million affected people.[1] The pathogenesis of RVO is characterized by thrombosis and obstruction within the retinal venous system, resulting from either retinal vein compression or vessel wall damage. Based on the site of the occlusion, RVO can be categorized as central RVO (CRVO) or branch RVO (BRVO). RVO may markedly impair retinal circulation, causing capillary damage that leads to complications such as macular edema (ME), neovascularization, retinal or vitreous hemorrhage, and eventually severe vision loss. RVO has been identified as a possible indicator of systemic vascular abnormalities, as conditions such as hypertension, hyperlipidemia, diabetes mellitus (DM), and atherosclerosis have been established as systemic risk factors for RVO.[1,2] Additionally, RVO patients also face an increased risk of cerebrovascular diseases.[2]

Optical coherence tomography angiography (OCTA) has been used to evaluate pathologic vascular changes in RVO[3–6]; however, several issues remain unresolved. Notably, alterations in the choroid associated with RVO have been poorly characterized, with conflicting findings regarding subfoveal choroidal thickness (SFCT) and flow density in the

choriocapillaris.[7,8] Additionally, there is also a lack of information about alterations in the large and medium choroidal vessels. Moreover, pathologic alterations in the fellow eyes of patients with RVO have been incompletely studied despite the systemic vascular associations of RVO, which might be expected to have impacts on the fellow eye. In prior studies, RVO fellow eyes were mainly used as controls or references for comparison against alterations evident in RVO eyes,[9–11] but these fellow eyes were not compared to healthy control eyes.[12] Furthermore, the choroidal vascularity index (CVI), a parameter calculated as the ratio of the choroidal luminal area to the total choroidal area in a single OCT B-scan, has recently been introduced to quantitatively analyze choroidal structure in the setting of various retinal diseases.[13] More recently, this two-dimensional (2D) CVI has been replaced by a three-dimensional (3D) CVI assessment using the entire OCT volume, but alterations in the 3D CVI in the setting of RVO have not been evaluated. Finally, most previous studies evaluating the retina and choroid using conventional OCTA were limited to a field of view (FOV) ranging from 3 × 3 mm to 12 × 12 mm,[14–16] without evaluating regions beyond the posterior pole, despite the fact that RVO commonly involves these more peripheral retinal regions. Given these gaps in knowledge, it would appear that a more comprehensive assessment of the retina and choroid using ultra-widefield imaging techniques would provide better insights into the angiographic and structural alterations and pathophysiology of RVO. In this study, we applied the novel ultra-widefield swept-source OCTA (UWF-SS-OCTA) with a FOV of 24 × 20 mm, which enabled visualization of the fundus beyond the posterior pole, allowing us to assess the peripheral retina and choroid in both RVO and RVO fellow eyes.

Methods

Study Design

This observational cross-sectional study was conducted in accordance with the tenets of the Declaration of Helsinki and was approved by the Ethics Committee of Peking Union Medical College Hospital (K3885). All included participants provided informed consent at enrollment.

Sample Size Calculation

Based on our preliminary evaluation, the mean foveal avascular zone (FAZ) area in the ischemic CRVO eyes and the healthy control eyes was found to be 0.50 and 0.30, respectively. With a type I error set at 0.05 and a power of 0.90, the minimum required sample size in each group was determined to be 12.[17]

Participant Enrollment

The CRVO and BRVO groups were each comprised of 15 unilateral RVO patients with the diagnosis confirmed by two experienced ophthalmologists (XZ, YC) at the Ophthalmology Department of Peking Union Medical College Hospital in Beijing, China, from August 2021 to May 2022. CRVO eyes exhibiting a deep capillary plexus (DCP) vessel density of ≤38.4% or retinal non-perfusion involving ≥10

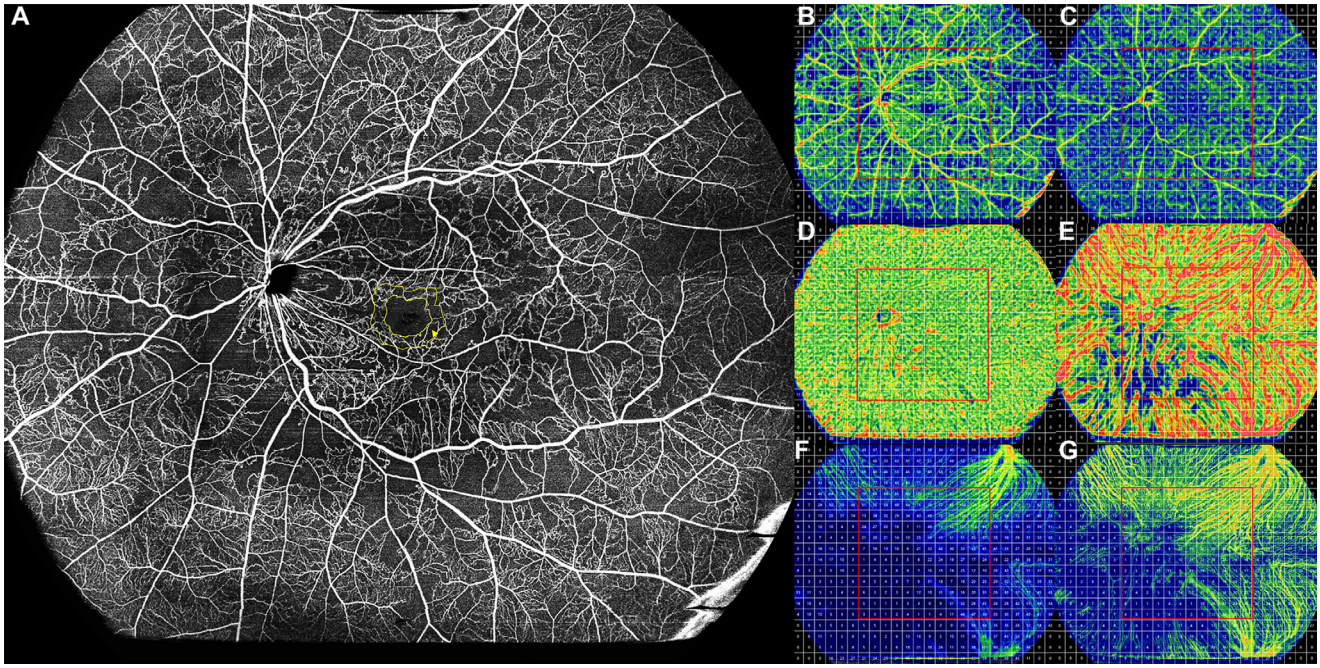

Figure 1. Schematic diagram of an ischemic CRVO participant. (**A**) Full retinal layer. All FAZ parameters, including the FAZ area, perimeter, AI, and FD-300, were measured on the full retinal layer (from the inner limiting membrane to 6 µm below the outer plexiform layer). FD-300 refers to the vessel flow density (VFD) in a 300-µm annulus surrounding the FAZ (*yellow arrowhead*). (**B–G**) The 24 × 20-mm UWF-SS-OCTA images of each retinal and choroidal layer were divided into 24 × 20 squares, each 1 × 1 mm, and each parameter was measured in the 1 × 1-mm square. The centered 12 × 12 squares were defined as the central region (*red box*), and other squares were defined as the peripheral region. (**B**) Superficial capillary plexus (SCP) layer, showing VFD. (**C**) DCP layer, showing VFD. (**D**) Choriocapillaris (CC) layer, showing VFD. (**E**) Large and medium choroidal vessel (LMCV) layer, showing VFD. (**F**) LMCV layer, showing choroidal vascularity volume (CVV). (**G**) LMCV layer, showing the CVI.

Investigative Ophthalmology & Visual Science

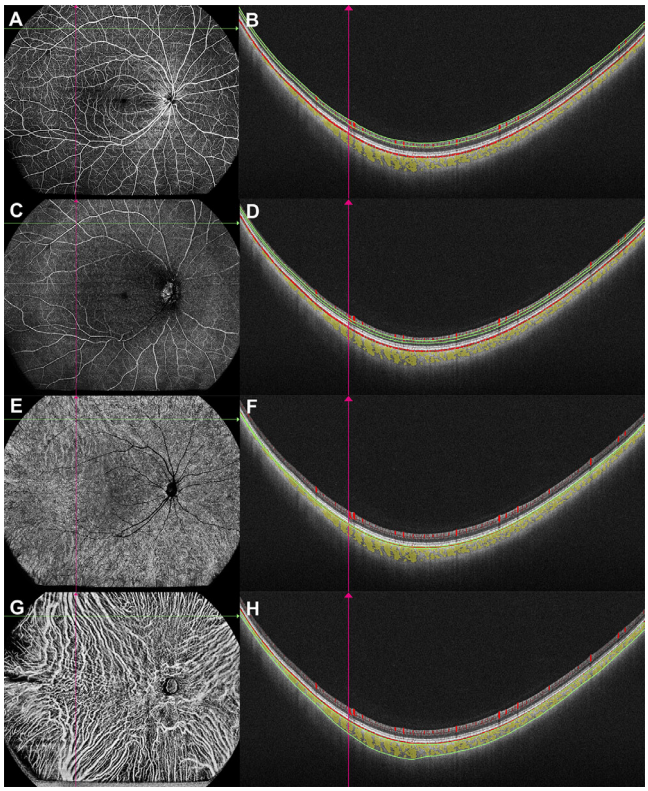

Figure 2. Schematic diagram of different retinal and choroidal sublayers in the UWF-SS-OCT and UWF-SS-OCTA images. In the UWF-SS-OCT images, the area marked in *red* represents the retinal vascularity and CC; the LMCV is marked in *yellow*; and the boundaries of sublayers are indicated by *green lines*. (**A**, **B**) SCP layer, from the inner limiting membrane to 9 µm below the inner plexiform layer. (**C**, **D**) DCP layer, from 6 µm below the inner plexiform layer to 9 µm below the outer plexiform layer. In the UWF-SS-OCTA images, the peripheral retinal arteries and veins remain visible in the DCP layer due to the thinner nature of the peripheral retina and the fact that the retinal vessels are partially situated in the DCP layer, rather than being caused by projection artifacts from SCP. This assertion finds support in the evident presence of retinal arteries and veins in the DCP layer as seen in the UWF-SS-OCT B-scan images. (**E**, **F**) CC layer, from Bruch's membrane to 29 µm below Bruch's membrane. (**G**, **H**) LMCV layer, from 29 µm below Bruch's membrane to the choroidoscleral interface.

disc areas in the acquired UWF-SS-OCTA images were categorized as ischemic CRVO.[18,19] The unaffected CRVO fellow and BRVO fellow eyes were also included. In addition, the healthy control group was comprised of 15 age-matched individuals without any ocular diseases (except for cataracts or non-pathologic myopia), with one eye randomly enrolled.

Exclusion criteria included the following:

1. Previous ocular treatment history, including intravitreal injection, laser therapy, or ocular surgery (except for cataract extraction)
2. Any other ocular comorbidities, such as diabetic retinopathy (DR), hypertensive retinopathy, retinal arterial occlusion, glaucoma, uveitis, etc. Participants with keratoconus, high myopia (≥−6.0 D), or high astigmatism (≥3 D) were also excluded.
3. Coexisting systemic diseases such as systemic autoimmune diseases that could be associated with RVO. In addition, DM cases were also excluded because patients with DM without clinically visible DR may also have abnormal fundus microcirculation.[20]
4. RVO-induced vitreous hemorrhage or pre- or intraretinal hemorrhage that could impair visualization of the retinal and choroidal vasculature
5. Participants with poor-quality OCTA images or incomplete medical records regarding their systemic history

All enrolled participants underwent comprehensive ophthalmic examinations, including assessments of best-corrected visual acuity (BCVA), intraocular pressure (IOP), slit-lamp examination, mydriatic ophthalmoscopy, UWF-SS-OCT, and UWF-SS-OCTA.

UWF-SS-OCTA Image Acquisition and Analysis

The UWF-SS-OCT and UWF-SS-OCTA images were captured using a BMizar (BM-400K) instrument (TowardPi Medical Technology, Beijing, China). It utilizes a 1060-nm-wavelength, swept-source vertical-cavity surface-emitting laser with a speed of 400,000 A-scans per second, providing a transverse resolution of 10 µm and an axial resolution of 3.8 µm. The A-scan depth within the tissue is 6.0 mm (2560 pixels). For UWF-SS-OCTA, a fovea-centered 24 × 20-mm scan pattern was chosen. This pattern consisted of 1536 A-scans per B-scan at 1280 B-scan positions, resulting in a 15.625-µm A-scan and B-scan separation. Central macular thickness (CMT) and SFCT were measured in UWF-SS-OCT images using instrument caliper tools. Two independent ophthalmologists (XZ, QZ) performed these measurements, and the mean value of each measurement was recorded. The FAZ was automatically identified in UWF-SS-OCTA images using the built-in instrument software, with errors manually corrected when required. FAZ-related parameters, including area, perimeter, AI, and flow density in a 300-µm annulus surrounding the FAZ (FD-300), were measured using the full retinal slab (from the inner limiting membrane to 6 µm below the outer plexiform layer) (Fig. 1A). The AI was defined as the ratio of the FAZ perimeter to the standard circular perimeter of the equal FAZ area.

The retina and choroid were automatically segmented into sublayers by the built-in instrument software (Fig. 2), with artifacts minimized by employing volumetric projection artifact removal approaches. The retinal sublayers included the superficial capillary plexus (SCP) and DCP, and the choroidal sublayers consisted of the choriocapillaris (CC) and the large and medium choroidal vessel (LMCV) layers. All of these segmentations were manually inspected and corrected as needed by two ophthalmologists (XZ, QZ) before any calculation. The acquired 24 × 20-mm UWF-SS-OCTA images of each layer were divided into 24 × 20 squares, each measuring 1 × 1 mm. The squares within the centered 12 × 12 region were defined as the central region, equivalent to the FOV of conventional 12 × 12 mm OCTA images. Squares outside this region were defined as the peripheral region (Figs. 1B–1G).

Retinal parameters, including vessel flow density (VFD), thickness, and volume, were measured within the SCP, DCP, and the full retina. VFD was calculated as the ratio of the area occupied by the blood vessels divided by the total image area.[21] Following skeletonization, vessel linear density (VLD), defined as the ratio of the length occupied by the blood vessels to the total area in the linearized vessel map,[22] was measured within the SCP. Choroidal parame-

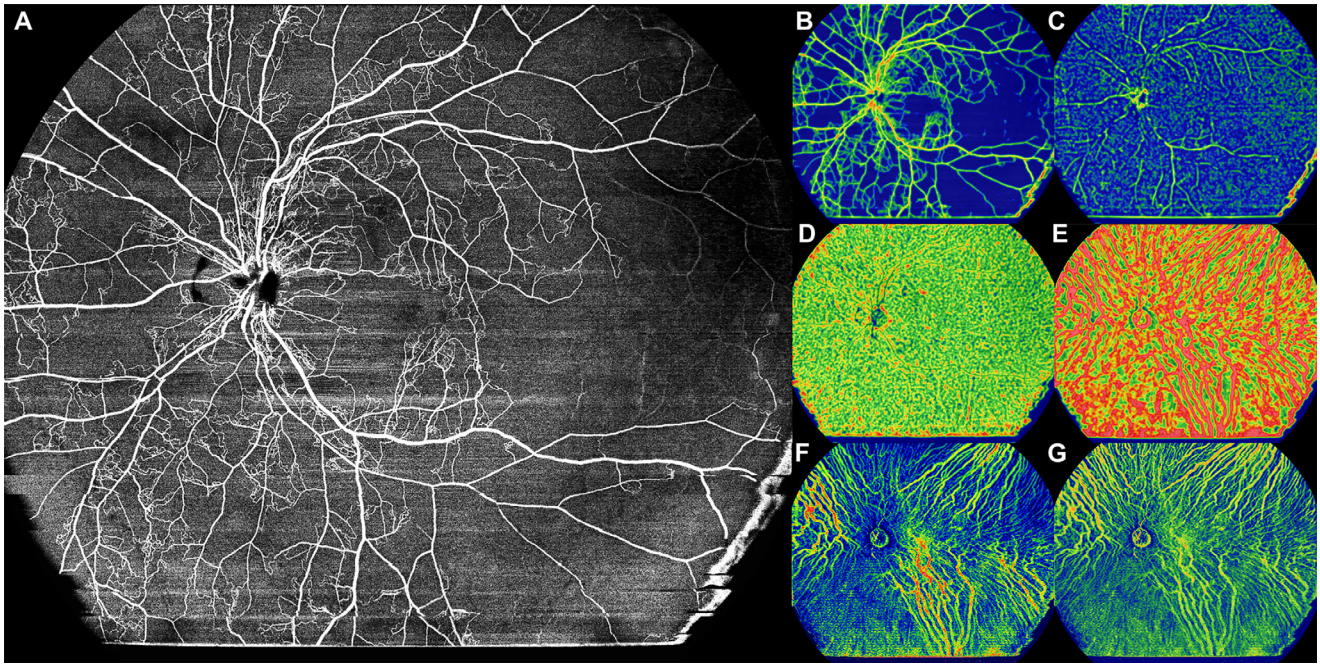

Figure 3. Representative UWF-SS-OCTA images of an ischemic CRVO participant. (**A**) Full retinal layer. (**B**) SCP layer, showing VFD. (**C**) DCP layer, showing VFD. (**D**) CC layer, showing VFD. (**E**) LMCV layer, showing VFD. (**F**) LMCV layer, showing CVV. (**G**) LMCV layer, showing the CVI.

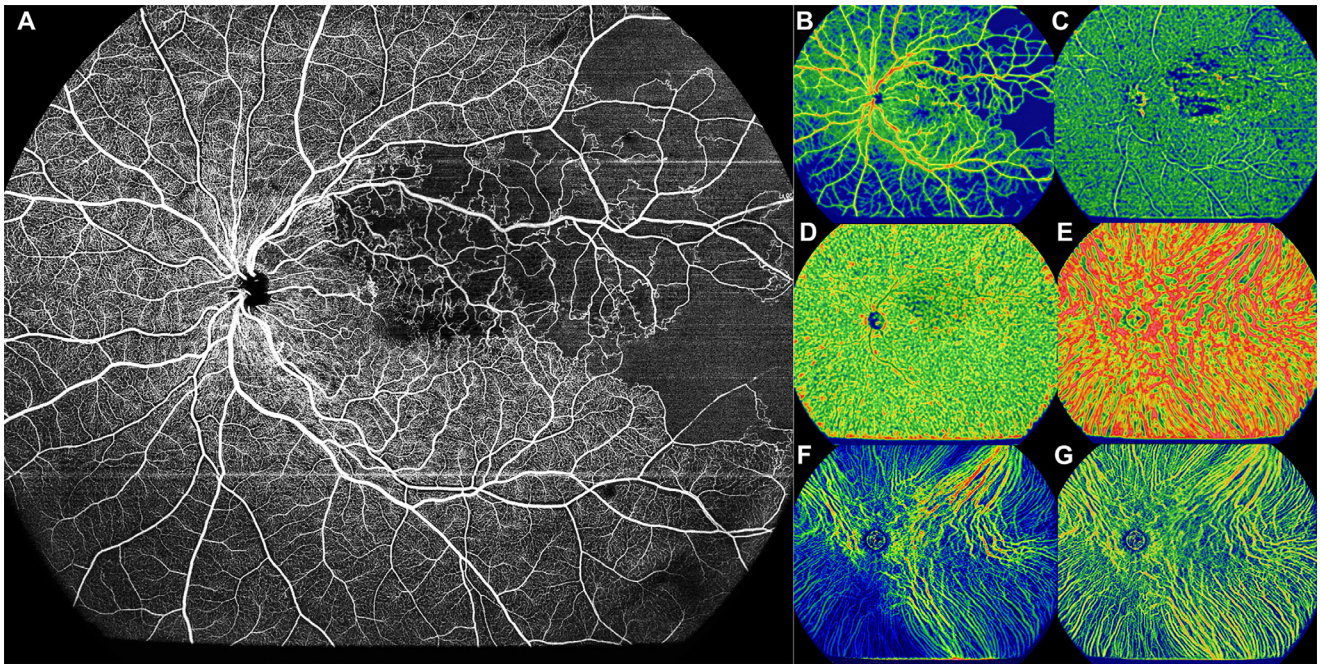

Figure 4. Representative UWF-SS-OCTA images of a BRVO participant. (**A**) Full retinal layer. (**B**) SCP layer, showing VFD. (**C**) DCP layer, showing VFD. (**D**) CC layer, showing VFD. (**E**) LMCV layer, showing VFD. (**F**) LMCV layer, showing CVV. (**G**) LMCV layer, showing the CVI.

ters measured from the UWF-SS-OCTA images included CC-VFD, LMCV-VFD, and choroidal vascularity volume (CVV) and CVI measured for the LMCV. CVV represents the volume of LMCV, and the CVI is the ratio of CVV to the total choroidal volume.[23] Each parameter was measured in the whole scan, central region, and peripheral region. Representative UWF-SS-OCTA images of CRVO and BRVO eyes are shown in Figures 3 and 4.

Data Analysis

Numerical and categorical data are displayed as mean ± SD and frequency (percentages), respectively. The Snellen BCVA was converted to the respective logMAR equivalent for statistical analysis.[24] The χ^2 test or Fisher's exact test was performed for comparisons of categorical variables. The dependent-variables *t*-test or Wilcoxon signed-rank test was

utilized to compare numerical data between the affected and unaffected eyes in RVO patients, depending on the data distribution. For the comparison of RVO and RVO fellow eyes with control eyes, the independent-variables *t*-test or Mann–Whitney *U* test was chosen. All statistical analyses were performed using Stata/SE 12.0 software (StataCorp, College Station, TX, USA), with $P < 0.05$ considered statistically significant.

Results

Demographic Characteristics

Participant demographics are summarized in Table 1. All 15 enrolled CRVO eyes (100.00%) met the criteria of a DCP vessel density of ≤38.4% or retinal non-perfusion involving ≥10 disc areas in the acquired UWF-SS-OCTA images, which qualified them for classification as ischemic CRVO. No hemi-RVO patients were identified. No statistically significant differences were observed in age, gender, IOP, spherical equivalent, or phakic status among the groups ($P > 0.05$). The average RVO durations in the ischemic CRVO and BRVO groups were 7.96 ± 10.43 and 6.56 ± 5.27 months, respectively. Ischemic CRVO and BRVO eyes had significantly worse BCVA compared to both fellow eyes and healthy control eyes ($P < 0.001$). Systemic hypertension was present in 13 ischemic CRVO patients (86.67%) and 12 BRVO patients (80.00%), but none was observed in controls ($P < 0.001$).

Retinal Parameters

A significantly increased area, perimeter, and AI of the FAZ were found in ischemic CRVO and BRVO eyes compared to fellow eyes and healthy control eyes ($P < 0.05$). Ischemic CRVO fellow and BRVO fellow eyes also had significantly higher AI than controls ($P < 0.05$). No statistically significant differences were present in CMT and FD-300 ($P > 0.05$).

Both affected and unaffected fellow eyes of ischemic CRVO and BRVO patients had significantly lower SCP-VFD than controls in the whole scan, peripheral region, and central region ($P < 0.05$). Additionally, ischemic CRVO eyes had lower peripheral SCP-VFD than their fellow eyes (26.14 ± 4.02 vs. 28.65 ± 1.25; $P = 0.029$). Significantly lower DCP and full retinal VFD were found in ischemic CRVO, ischemic CRVO fellow, and BRVO eyes than in controls ($P < 0.05$). Comparison of DCP VFD and full retinal VFD in central and peripheral regions recapitulated these findings, with the exception of no difference in central retinal VFD between ischemic CRVO fellow eyes and control eyes ($P > 0.05$). BRVO fellow eyes had a lower central DCP VFD than controls (31.09 ± 3.19 vs. 34.32 ± 5.11; $P = 0.047$). The SCP-VLD in ischemic CRVO and BRVO eyes was significantly lower than in their fellow eyes and controls across the whole scan areas of UWF-SS-OCTA images ($P < 0.05$).

The affected and unaffected fellow eyes of ischemic CRVO and BRVO patients had significantly increased thickness and volume in the SCP, DCP, and the full retina ($P < 0.05$) compared to controls, except for no difference in SCP thickness between BRVO fellow eyes and control eyes ($P > 0.05$). When comparing BRVO eyes with BRVO fellow eyes, greater thickness in the DCP and full retina and a higher volume in all retinal layers were observed in the BRVO eyes ($P < 0.05$). The comparisons of retinal parameters among groups are summarized in Table 2.

Table 1. Demographics of the Participants

Variable	Control ($n = 15$)	Ischemic CRVO ($n = 15$)				BRVO ($n = 15$)				
		Ischemic CRVO Eyes	*P* vs. Control	*P* vs. Fellow	Fellow Eyes	*P* vs. Control	BRVO Eyes	*P* vs. Control	*P* vs. Fellow	Fellow Eyes	*P* vs. Control
Age (y), mean ± SD	49.83 ± 9.14	51.92 ± 17.44	0.684		51.92 ± 17.44	0.684	55.50 ± 14.18	0.204		55.50 ± 14.18	0.204
Male gender, *n* (%)	7 (46.67)	8 (53.33)	0.715		8 (53.33)	0.715	7 (46.67)	1.000		7 (46.67)	1.000
RVO duration (mo), mean ± SD		7.96 ± 10.43					6.56 ± 5.27				
BCVA, mean ± SD	0.86 ± 0.23	0.25 ± 0.28	<0.001*	<0.001*	0.67 ± 0.29	0.058	0.46 ± 0.30	<0.001*	<0.001*	0.88 ± 0.18	0.793
IOP (mmHg), mean ± SD	16.11 ± 3.41	17.15 ± 8.11	0.660	0.341	14.67 ± 5.51	0.399	14.87 ± 2.03	0.236	0.419	15.38 ± 1.25	0.439
Spherical equivalent (D), mean ± SD	−2.20 ± 1.58	−1.31 ± 1.25	0.098	0.944	−1.28 ± 1.08	0.073	−1.23 ± 1.13	0.063	0.815	−1.32 ± 0.95	0.075
Pseudophakia (eyes), *n* (%)	0 (0.00)	2 (13.33)	0.483		1 (6.67)	1.000	0 (0.00)	NA		1 (6.67)	1.000
Systemic comorbidity, *n* (%)											
Hypertension	0 (0.00)	13 (86.67)	<0.001*		13 (86.67)	<0.001*	12 (80.00)	<0.001*		12 (80.00)	<0.001*
Diabetes mellitus	0 (0.00)	0 (0.00)	NA		0 (0.00)	NA	0 (0.00)	NA		0 (0.00)	NA
Hyperlipidemia	0 (0.00)	6 (40.00)	0.022*		6 (40.00)	0.022*	4 (26.67)	0.050		4 (26.67)	0.050

*$P < 0.05$.

Table 2. Retinal Parameters of RVO, Fellow, and Healthy Control Eyes

		Ischemic CRVO ($n = 15$)					BRVO ($n = 15$)				
Variable	**Control ($n = 15$)**	**Ischemic CRVO Eyes**	***P* vs. Control**	***P* vs. Fellow**	**Fellow Eyes**	***P* vs. Control**	**BRVO Eyes**	***P* vs. Control**	***P* vs. Fellow**	**Fellow Eyes**	***P* vs. Control**
CMT (μm), mean ± SD	232.37 ± 24.52	301.46 ± 155.57	0.102	0.224	241.33 ± 105.55	0.752	241.19 ± 128.34	0.796	0.901	237.00 ± 10.81	0.509
FAZ, mean ± SD											
Area (mm^2)	0.32 ± 0.13	0.53 ± 0.33	0.031*	0.006*	0.26 ± 0.12	0.168	0.45 ± 0.16	0.023*	0.010*	0.32 ± 0.10	0.837
Perimeter (mm)	2.34 ± 0.58	3.45 ± 1.22	0.003*	0.002*	2.02 ± 0.41	0.092	2.89 ± 0.68	0.024*	0.032*	2.41 ± 0.47	0.718
AI	1.20 ± 0.08	1.39 ± 0.20	0.002*	<0.001*	1.28 ± 0.08	0.013*	1.33 ± 0.09	<0.001*	0.032*	1.26 ± 0.08	0.049*
FD-300 (%)	0.31 ± 0.06	0.29 ± 0.05	0.287	0.550	0.30 ± 0.04	0.596	0.30 ± 0.06	0.598	0.624	0.31 ± 0.05	0.999
VFD (%), mean ± SD											
SCP											
Whole scan	33.96 ± 3.12	29.13 ± 5.19	0.005*	0.134	31.24 ± 1.07	0.004*	30.33 ± 5.95	0.046*	0.473	31.58 ± 2.97	0.041*
Central region	39.83 ± 3.21	35.70 ± 5.21	0.014*	0.221	37.52 ± 2.15	0.028*	36.43 ± 4.69	0.028*	0.216	38.01 ± 1.15	0.048*
Peripheral region	30.88 ± 3.24	26.14 ± 4.02	0.001*	0.029*	28.65 ± 1.25	0.019*	27.88 ± 4.16	0.036*	0.321	29.010 ± 1.22	0.046*
DCP											
Whole scan	31.44 ± 4.89	25.703 ± 7.01	0.015*	0.115	28.19 ± 3.50	0.046*	26.65 ± 6.13	0.025*	0.226	29.03 ± 4.23	0.160
Central region	34.32 ± 5.11	27.28 ± 7.78	0.007*	0.088	31.10 ± 3.11	0.046*	28.71 ± 5.99	0.010*	0.185	31.09 ± 3.19	0.047*
Peripheral region	28.78 ± 3.84	24.78 ± 5.75	0.033*	0.475	26.01 ± 3.19	0.040*	25.29 ± 5.35	0.0496*	0.363	27.01 ± 4.82	0.275
Retina											
Whole scan	33.91 ± 3.39	30.11 ± 5.44	0.029*	0.515	31.16 ± 2.90	0.024*	30.55 ± 5.12	0.043*	0.355	32.04 ± 3.37	0.141
Central region	39.16 ± 3.29	34.79 ± 5.35	0.012*	0.062	37.83 ± 2.82	0.245	35.51 ± 5.68	0.040*	0.141	37.94 ± 2.51	0.263
Peripheral region	31.16 ± 3.57	25.28 ± 5.80	0.002*	0.115	28.04 ± 3.07	0.016*	26.81 ± 6.42	0.030*	0.232	29.13 ± 3.58	0.131
VLD (%), mean ± SD											
SCP											
Whole scan	8.52 ± 0.82	7.28 ± 1.31	0.004*	0.007*	8.30 ± 0.29	0.331	7.29 ± 1.64	0.015*	0.016*	8.52 ± 0.89	0.999
Central region	9.89 ± 0.78	8.97 ± 1.25	0.022*	0.129	9.53 ± 0.60	0.166	8.84 ± 1.60	0.031*	0.009*	10.10 ± 0.67	0.436
Peripheral region	7.81 ± 0.87	6.51 ± 1.43	0.006*	0.004*	7.70 ± 0.19	0.658	6.59 ± 1.66	0.018*	0.026*	7.75 ± 0.94	0.862
Thickness (μm), mean ± SD											
SCP											
Whole scan	65.53 ± 4.31	85.18 ± 10.94	<0.001*	0.096	79.15 ± 8.02	<0.001*	77.52 ± 9.84	<0.001*	0.007*	68.97 ± 5.73	0.074
Central region	65.37 ± 8.45	119.62 ± 19.99	<0.001*	0.395	113.19 ± 20.75	<0.001*	109.38 ± 21.13	<0.001*	0.043*	97.35 ± 5.99	<0.001*
Peripheral region	65.60 ± 5.09	70.83 ± 8.08	0.043*	0.008*	64.56 ± 2.68	0.490	63.87 ± 7.56	0.467	0.008*	56.80 ± 5.89	<0.001*
DCP											
Whole scan	157.40 ± 8.90	176.42 ± 14.00	<0.001*	0.576	179.15 ± 12.36	<0.001*	177.23 ± 14.53	<0.001*	0.028*	168.02 ± 5.06	<0.001*
Central region	155.93 ± 5.21	192.99 ± 19.27	<0.001*	0.220	201.16 ± 16.27	<0.001*	194.76 ± 17.56	<0.001*	0.001*	177.991 ± 3.32	<0.001*
Peripheral region	158.03 ± 10.98	169.31 ± 13.78	0.019*	0.934	169.71 ± 12.45	0.011*	169.72 ± 18.43	0.044*	0.254	163.76 ± 7.39	0.105

Table 2. Continued

Variable	Control ($n = 15$)	Ischemic CRVO ($n = 15$)					BRVO ($n = 15$)				
		Ischemic CRVO Eyes	*P* vs. Control	*P* vs. Fellow	Fellow Eyes	*P* vs. Control	BRVO Eyes	*P* vs. Control	*P* vs. Fellow	Fellow Eyes	*P* vs. Control
Retina											
Whole scan	222.93 ± 9.37	261.60 ± 22.60	<0.001*	0.665	258.31 ± 18.29	<0.001*	254.75 ± 21.00	<0.001*	0.004*	236.99 ± 5.69	<0.001*
Central region	221.30 ± 10.61	312.61 ± 37.49	<0.001*	0.897	314.37 ± 36.19	<0.001*	304.13 ± 35.32	<0.001*	0.004*	275.34 ± 7.43	<0.001*
Peripheral region	223.62 ± 12.34	239.74 ± 19.32	0.011*	0.385	234.29 ± 14.09	0.036*	233.58 ± 23.47	0.157	0.049*	220.56 ± 7.06	0.411
Volume (mm^3), mean ± SD											
SCP											
Whole scan	0.065 ± 0.004	0.084 ± 0.011	<0.001*	0.089	0.078 ± 0.008	<0.001*	0.077 ± 0.010	<0.001*	0.007*	0.068 ± 0.005	0.041*
Central region	0.065 ± 0.008	0.120 ± 0.020	<0.001*	0.403	0.113 ± 0.021	<0.001*	0.109 ± 0.021	<0.001*	0.042*	0.097 ± 0.006	<0.001*
Peripheral region	0.065 ± 0.005	0.069 ± 0.008	0.098	0.011*	0.063 ± 0.002	0.209	0.063 ± 0.007	0.389	0.008*	0.056 ± 0.005	<0.001*
DCP											
Whole scan	0.155 ± 0.010	0.173 ± 0.015	0.001*	0.676	0.175 ± 0.012	<0.001*	0.175 ± 0.016	<0.001*	0.078	0.166 ± 0.007	0.001*
Central region	0.155 ± 0.005	0.193 ± 0.019	<0.001*	0.225	0.201 ± 0.016	<0.001*	0.195 ± 0.017	<0.001*	0.001*	0.178 ± 0.003	<0.001*
Peripheral region	0.155 ± 0.013	0.164 ± 0.016	0.078	0.936	0.164 ± 0.012	0.055	0.166 ± 0.021	0.091	0.470	0.161 ± 0.010	0.129
Retina											
Whole scan	0.220 ± 0.010	0.257 ± 0.024	<0.001*	0.613	0.253 ± 0.018	<0.001*	0.251 ± 0.022	<0.001*	0.009*	0.235 ± 0.006	<0.001*
Central region	0.221 ± 0.011	0.313 ± 0.038	<0.001*	0.906	0.314 ± 0.036	<0.001*	0.304 ± 0.035	<0.001*	0.004*	0.275 ± 0.007	<0.001*
Peripheral region	0.219 ± 0.014	0.233 ± 0.021	0.046*	0.343	0.227 ± 0.014	0.148	0.228 ± 0.026	0.238	0.127	0.218 ± 0.009	0.655

* $P < 0.05$.

Investigative Ophthalmology & Visual Science

Table 3. Choroidal Parameters of the RVO, Fellow, and Healthy Control Eyes

Variable	Control (n = 15)	Ischemic CRVO (n = 15)			BRVO (n = 15)			
		Eyes	P vs. Control	P vs. Fellow	Fellow Eyes	P vs. Control	BRVO Eyes	P vs. Control	P vs. Fellow	Fellow Eyes	P vs. Control
SFCT (μm), mean ± SD	236.90 ± 77.81	223.92 ± 119.57	0.728	0.357	261.33 ± 94.50	0.447	264.81 ± 138.24	0.501	0.887	270.83 ± 83.60	0.260
CC-VFD (%), mean ± SD											
Whole scan	43.54 ± 1.12	43.33 ± 0.99	0.594	0.697	43.13 ± 1.54	0.414	42.84 ± 1.28	0.119	0.399	43.14 ± 0.52	0.219
Central region	45.48 ± 0.81	45.97 ± 1.51	0.264	0.283	45.45 ± 1.05	0.922	45.16 ± 1.25	0.412	0.765	45.27 ± 0.66	0.443
Peripheral region	42.57 ± 1.52	42.09 ± 1.23	0.360	0.949	42.05 ± 2.04	0.528	41.76 ± 1.69	0.179	0.630	42.09 ± 0.88	0.298
LMCV-VFD (%), mean ± SD											
Whole scan	63.84 ± 2.55	60.14 ± 4.04	0.006*	0.108	62.04 ± 1.81	0.035*	60.11 ± 5.70	0.028*	0.040*	63.47 ± 2.04	0.669
Central region	68.29 ± 2.15	64.52 ± 6.06	0.031*	0.133	67.33 ± 3.49	0.372	65.06 ± 5.15	0.033*	0.140	67.25 ± 2.51	0.233
Peripheral region	61.52 ± 3.14	58.75 ± 4.06	0.020*	0.513	59.49 ± 1.49	0.003*	58.57 ± 4.11	0.036*	0.039*	60.96 ± 2.04	0.570
CVV (mm^3), mean ± SD											
Whole scan	72.87 ± 15.22	65.13 ± 24.27	0.305	0.976	64.85 ± 26.67	0.321	82.89 ± 41.03	0.383	0.464	74.32 ± 17.82	0.813
Central region	81.68 ± 17.52	77.05 ± 32.45	0.602	0.574	70.16 ± 33.84	0.252	95.00 ± 48.81	0.328	0.338	81.88 ± 18.12	0.976
Peripheral region	68.21 ± 15.00	62.62 ± 21.94	0.456	0.981	62.43 ± 23.67	0.431	77.09 ± 36.81	0.399	0.542	70.55 ± 18.055	0.702
CVI (%), mean ± SD											
Whole scan	30.94 ± 3.68	27.78 ± 4.66	0.049*	0.290	26.31 ± 2.47	<0.001*	29.63 ± 5.16	0.432	0.524	30.74 ± 4.16	0.890
Central region	34.41 ± 4.34	30.29 ± 4.55	0.018*	0.158	28.08 ± 3.69	<0.001*	31.19 ± 4.12	0.047*	0.197	33.03 ± 3.48	0.343
Peripheral region	29.02 ± 3.87	26.60 ± 4.31	0.116	0.335	25.47 ± 1.99	0.004*	28.25 ± 5.02	0.645	0.450	29.59 ± 4.55	0.715

* $P < 0.05$.

Choroidal Parameters

Ischemic CRVO and BRVO eyes had significantly decreased LMCV-VFD compared with control eyes in the whole scan, central, and peripheral regions ($P < 0.05$). Lower whole scan and peripheral LMCV-VFD values were also found for ischemic CRVO fellow eyes versus control eyes, and for BRVO eyes versus BRVO fellow eyes ($P > 0.05$). Both ischemic CRVO and ischemic CRVO fellow eyes had significantly lower whole and central CVI values compared to controls ($P < 0.05$). Lower peripheral CVI values were also observed for ischemic CRVO fellow eyes compared to control eyes (25.47 ± 1.99 vs. 29.02 ± 3.87; $P = 0.004$). In addition, the central CVI in BRVO eyes was 31.19 ± 4.12, which was significantly lower than in control eyes (34.41 ± 4.34; $P = 0.047$). No significant differences existed in SFCT, CC-VFD, and CVV among these groups ($P > 0.05$) (Table 3).

Discussion

The present study is the first, to the best of our knowledge, to utilize UWF-SS-OCTA to evaluate both retinal and choroidal alterations in the central and peripheral regions of RVO and RVO fellow eyes. Our findings indicate that both ischemic CRVO and BRVO eyes showed FAZ enlargement and irregularity; we also detected FAZ irregularity in ischemic CRVO fellow and BRVO fellow eyes. Both the affected and unaffected eyes of ischemic CRVO and BRVO patients had decreased VFD, increased thickness, and increased volume in the central and/or peripheral retinal regions. Lower LMCV-VFD and CVI were also observed in ischemic CRVO, ischemic CRVO fellow, and BRVO eyes.

The FAZ is the macular capillary-free zone surrounded by interconnected capillaries, with an average area of 0.20 to 0.40 mm^2 in healthy individuals.[25] Wons et al.[26] reported that the size of FAZ may be an indicator of the status of foveal circulation in retinal vasculopathy. In the present study, ischemic CRVO and BRVO eyes had increased FAZ area and perimeter compared to both fellow eyes and controls, which is consistent with previous findings.[26–28] The AI is a recently introduced parameter to evaluate deviation of the FAZ shape from a perfect circle. Deng et al.[29] found that CRVO eyes had significantly higher AI than controls. Similarly, our study reported increased AI in both ischemic CRVO and BRVO eyes compared to their fellow eyes and healthy control eyes. In addition, we found significantly decreased VFD in ischemic CRVO and BRVO eyes in the SCP, DCP, and full retina compared with the healthy control eyes, consistent with previous findings.[11,30–33] It should be noted that the DCP is the principal venous outflow system for the retinal capillary plexuses, and collateral vessels typically develop in the DCP during the evolution of RVO.[34] Previous investigations have pointed out that the development of these collateral vessels is negatively associated with retinal VFD.[35] RVO could impair retinal venous outflow, cause dilation and tortuosity of vascular segments, and increase the retinal capillary pressure. These various pathologic alterations may promote the exudation of blood and fluid into the intercellular space,[36] which might explain the increased retinal thickness and volume observed in RVO eyes compared to healthy control eyes in our study.

The choroid, containing the most extensive vasculature in the eye, plays a critical role in supplying oxygen and nutrition to the outer retinal layers. Given the interactions

between the retina and the choroid, it is perhaps not surprising that RVO may have an impact on the choroid. Previous studies on SFCT in RVO eyes have yielded inconsistent results, with several reporting increased SFCT in RVO eyes[8,37–39] and others finding no difference between RVO and their fellow eyes.[14,40,41] Our study found a similar SFCT in ischemic CRVO and BRVO eyes compared to their fellow eyes and controls. Whether RVO could impact the CC-VFD is also a topic of controversy. Some OCTA studies have observed lower CC-VFD in RVO eyes than their fellow eyes and control eyes and the utilization of anti-vascular endothelial growth factor (VEGF) agents could normalize the CC-VFD.[9,42,43] Nevertheless, other studies found similar CC-VFD in CRVO and BRVO eyes compared to their respective fellow eyes.[15,44] In our analysis using UWF-SS-OCTA, no differences were observed in CC-VFD in ischemic CRVO and BRVO eyes compared to their fellow eyes and control eyes. Although the reasons for the discordant findings regarding the choroid in RVO among these various studies are not well understood, we speculate that differences in gender, axial length, type and stage of RVO, and RVO-associated complications such as ME may play a role.

Aribas et al.[9] proposed that the size of larger choroidal vessels was either not influenced or only slightly increased in RVO eyes, based on an evaluation of the ratio of the thickness of the Haller layer to the whole choroid,. In this study, we introduced a novel three-dimensional parameter, CVV, to gain a more comprehensive understanding of structural alterations in the LMCV in RVO eyes. Our findings showed that the CVVs in ischemic CRVO and BRVO eyes were similar to their fellow eyes and control eyes. The CVI is a two-dimensional parameter introduced in previous studies to quantitatively analyze choroidal composition and was defined as the ratio of choroidal luminal area to the total choroidal area in OCT B-scans.[45] A lower 2D CVI was observed in RVO eyes compared to their fellow eyes and controls.[9,13,45] Hwang et al.[13] further noted that the CVI in BRVO eyes increased and became similar to that of their fellow eyes after intravitreal injection of anti-VEGF agents. In our study, we computed a more comprehensive 3D CVI as the ratio of CVV to total choroidal volume. Using this 3D approach, we noted that ischemic CRVO eyes had significantly lower CVI values than healthy control eyes in the whole OCTA image and the central region. In addition, BRVO eyes exhibited lower 3D CVI values than healthy control eyes in the central choroidal region, although not in the whole scan or the peripheral region.

However, the underlying mechanisms and pathogenesis behind the decreased CVI in RVO eyes remain unclear. The decreased CVI with unchanged CVV in RVO eyes may imply an increased choroidal stromal volume, which may suggest the possibility of choroidal swelling or congestion affecting the stroma. The lower LMCV-VFD in ischemic CRVO and BRVO eyes compared with healthy control eyes might also be explained by the increased choroidal stromal volume. Previous studies have reported that the impaired venous flow in RVO may cause blood and fluid exudation into the intercellular space.[36] We speculate that impaired retinal venous outflow may promote extracellular fluid movement toward the choroid, contributing to choroidal stroma swelling and an increase in volume. An alternative hypothesis is that the ischemia-induced production of VEGF may also impact the adjacent choroid, leading to increased choroidal vascular fluid leakage and attendant choroidal stromal edema.[46] Julien et al.[47] found that anti-VEGF agents could reduce the number of choriocapillaris endothelial cell fenestrations in monkeys. This finding might suggest that anti-VEGF agents have the potential to reduce fluid leakage through fenestrated vascular walls, possibly thereby relieving choroidal stromal swelling. Mitamura et al.[48] did find that intravitreal aflibercept injection could significantly reduce the choroidal stromal area in RVO eyes. The observation of a decreased CVI with unchanged CVV in the unaffected fellow eyes of RVO patients compared to healthy control eyes raises the possibility that the reduced CVI might also be attributed to systemic conditions, such as hypertension or other cardiovascular risk factors. Whether isolated choroidal stromal expansion is specific to RVO or may be observed in other conditions requires further study. It is notable that eyes with central serous chorioretinopathy typically feature choroidal luminal expansion,[49] but diabetic ME is associated with increased luminal and stromal volumes.[50]

Our findings revealed notable alterations in the retina and choroid of the unaffected fellow eyes of RVO patients. For example, ischemic CRVO fellow eyes were associated with significantly decreased retinal VFD, increased retinal thickness and volume, increased LMCV-VFD, and decreased CVI compared to healthy controls. These findings align with previous research by Park et al.,[10] who also reported microvascular impairment in the retina and choroid of RVO fellow eyes. Collectively, these results lend support to the hypothesis that RVO is not solely a localized ocular event but may instead be indicative of broader systemic vascular changes affecting both eyes. The observed retinal microvascular impairment in RVO eyes could arise from a combination of the influence of systemic risk factors prior to the onset of occlusion and the non-perfusion area that develops after vein occlusion. A meta-analysis conducted by Song et al.[1] reported various systemic factors associated with a higher risk of RVO, such as advanced age, hypertension, myocardial infarction, stroke, higher total cholesterol, and higher creatinine. Therefore, it may be speculated that the management of systemic factors may be relevant to preventing the progression of RVO.

The utilization of UWF-SS-OCTA imaging in this study allowed for the comprehensive visualization of both central and peripheral fundus regions in a single examination. For example, we noticed that, compared to controls, ischemic CRVO fellow eyes had significantly lower peripheral LMCV-VFD, but no significant difference existed in the central region. In BRVO eyes, a lower LMCV-VFD than in their fellow eyes was found in the peripheral region but not in the central region, which would typically be the only region evaluated by conventional OCTA imaging. The importance of employing UWF imaging assessments has also emerged in other retinal vascular diseases, such as in DR, where peripheral lesions are thought to be of prognostic importance and may impact future staging systems for DR.[51,52] UWF-SS-OCTA, enabling the visualization of the peripheral fundus region, is a promising imaging technique to characterize the retinal and choroid vasculature.

In OCTA images, minimizing volumetric projection artifacts from the SCP is crucial for achieving clear visualization and accurate quantification of vessel flow in the outer retinal layers, particularly in the DCP layer. In our study, we observed that the peripheral retinal arteries and veins remained visible in the DCP layer of UWF-SS-OCTA images. This finding is consistent with the report by Hormel et al. (*IOVS* 2023;64(8):ARVO E-Abstract 4422), who also observed the visualization of peripheral retinal arteries and veins in

UWF-SS-OCTA images. The visibility of these vessels in the DCP layer can be attributed to the thinner nature of the peripheral retina and the partial location of retinal vessels within the DCP layer, rather than as a result of projection artifacts from SCP. Further supporting this explanation is the clear presence of retinal arteries and veins in the DCP layer, as demonstrated in the UWF-SS-OCT B-scan images of our study.

Fluorescein angiography has traditionally served as the standard imaging modality for assessing retinal perfusion in cases of RVOs within clinical practice, but it presents important limitations, including invasiveness, time-consuming procedures, and the potential for severe systemic risks. The introduction of OCTA has revolutionized the non-invasive evaluation of fundus vasculature, eliminating the need for invasive dye administration.[53] Our study found that OCTA could offer clear visualization of non-perfusion areas in RVO-affected eyes, demonstrating its potential to distinguish between ischemic and non-ischemic RVO cases. This distinction is invaluable for informing the prognosis and guiding the management of RVO. Furthermore, OCTA provides depth-resolved angiographic images, enabling quantitative analysis of choroidal sublayers, which are largely overlooked in fluorescein angiography. Our study, utilizing the innovative UWF-SS-OCTA, has revealed specific choroidal alterations in RVO eyes that have the potential to ignite researchers' interest in further exploring the relationship between these alterations and the progression of RVO in prospective studies. These choroidal alterations could potentially serve as prognostic parameters for the effective management of RVO cases. Moreover, the notable retinal and choroidal alterations observed in the unaffected fellow eyes of RVO patients suggest a link between RVO and systemic vascular changes and underscore the importance of systemic management for RVO patients in clinical practice.

Our study is not without limitations that should be considered when assessing our findings. First, our sample size was relatively small; thus, we may have been underpowered to detect small differences in parameters between groups. However, despite this, a number of significant differences, including those between fellow eyes and healthy control eyes, were observed. Second, as this was a hospital-based study, the population, particularly the healthy controls, may not reflect the broader community. Third, RVO patients included in this study only underwent single timepoint OCTA imaging, and this may have occurred at different time points following the RVO diagnosis. Variability in disease duration may impact our results, as longitudinal alterations in the circulation may affect these patients. Further prospective longitudinal studies with larger study populations will be necessary to address these limitations. Nonetheless, we believe our findings underscore the importance and value of widefield SS-OCTA imaging.

In conclusion, the affected and unaffected fellow eyes of RVO patients showed both central and/or peripheral structural and vascular changes affecting the retina and choroid. UWF-OCTA, enabling the visualization of the more peripheral fundus regions, offers a promising approach to more fully characterize vascular alterations in RVO.

Acknowledgments

Supported by research grants from the Fundamental Research Funds for the Central Universities (3332022008) and the National College Students Innovation and Entrepreneurship Training Program (2023zglc06014).

Disclosure: **X. Zhao**, None; **Q. Zhao**, None; **C. Wang**, None; **L. Meng**, None; **S. Cheng**, None; **X. Gu**, None; **S.R. Sadda**, None; **Y. Chen**, None

References

1. Song P, Xu Y, Zha M, Zhang Y, Rudan I. Global epidemiology of retinal vein occlusion: a systematic review and meta-analysis of prevalence, incidence, and risk factors. *J Glob Health*. 2019;9(1):010427.
2. Jaulim A, Ahmed B, Khanam T, Chatziralli IP. Branch retinal vein occlusion: epidemiology, pathogenesis, risk factors, clinical features, diagnosis, and complications. An update of the literature. *Retina*. 2013;33(5):901–910.
3. Kashani AH, Chen CL, Gahm JK, et al. Optical coherence tomography angiography: a comprehensive review of current methods and clinical applications. *Prog Retin Eye Res*. 2017;60:66–100.
4. Kang JW, Yoo R, Jo YH, Kim HC. Correlation of microvascular structures on optical coherence tomography angiography with visual acuity in retinal vein occlusion. *Retina*. 2017;37(9):1700–1709.
5. Ryu G, Park D, Lim J, van Hemert J, Sagong M. Macular microvascular changes and their correlation with peripheral nonperfusion in branch retinal vein occlusion. *Am J Ophthalmol*. 2021;225:57–68.
6. Sakimoto S, Kawasaki R, Nishida K. Retinal neovascularization-simulating retinal capillary reperfusion in branch retinal vein occlusion, imaged by wide-field optical coherence tomography angiography. *JAMA Ophthalmol*. 2020;138(2):216–218.
7. Khodabandeh A, Shahraki K, Roohipoor R, et al. Quantitative measurement of vascular density and flow using optical coherence tomography angiography (OCTA) in patients with central retinal vein occlusion: can OCTA help in distinguishing ischemic from non-ischemic type? *Int J Retina Vitreous*. 2018;4:47.
8. Rayess N, Rahimy E, Ying GS, et al. Baseline choroidal thickness as a predictor for treatment outcomes in central retinal vein occlusion. *Am J Ophthalmol*. 2016;171:47–52.
9. Aribas YK, Hondur AM, Tezel TH. Choroidal vascularity index and choriocapillary changes in retinal vein occlusions. *Graefes Arch Clin Exp Ophthalmol*. 2020;258(11):2389–2397.
10. Park YJ, Kim J, Lee EJ, Park KH. Peripapillary microvascular of the retina and choriocapillaris in uninvolved fellow eyes of unilateral retinal vein occlusion patients. *Retina*. 2022;42(1):159–167.
11. Fan L, Zhu Y, Liao R. Evaluation of macular microvasculature and foveal avascular zone in patients with retinal vein occlusion using optical coherence tomography angiography. *Int Ophthalmol*. 2022;42(1):211–218.
12. Shin YI, Nam KY, Lee SE, et al. Changes in peripapillary microvasculature and retinal thickness in the fellow eyes of patients with unilateral retinal vein occlusion: an OCTA study. *Invest Ophthalmol Vis Sci*. 2019;60(2):823–829.
13. Hwang BE, Kim M, Park YH. Role of the choroidal vascularity index in branch retinal vein occlusion (BRVO) with macular edema. *PLoS One*. 2021;16(10):e0258728.
14. Loiudice P, Covello G, Figus M, Posarelli C, Sartini MS, Casini G. Choroidal vascularity index in central and branch retinal vein occlusion. *J Clin Med*. 2022;11(16):4756.
15. Chen L, Yuan M, Sun L, Chen Y. Three-dimensional analysis of choroidal vessels in the eyes of patients with unilateral BRVO. *Front Med (Lausanne)*. 2022;9:854184.

16. Deng Y, Cai X, Zhang S, et al. Quantitative analysis of retinal microvascular changes after conbercept therapy in branch retinal vein occlusion using optical coherence tomography angiography. *Ophthalmologica*. 2019;242(2):69–80.
17. Chow SC SJ, Wang H. *Sample Size Calculation in Clinical Research*. New York: Marcel Dekker; 2008.
18. An W, Zhao Q, Yu R, Han J. The role of optical coherence tomography angiography in distinguishing ischemic versus non-ischemic central retinal vein occlusion. *BMC Ophthalmol*. 2022;22(1):413.
19. Central Vein Occlusion Study Group. Natural history and clinical management of central retinal vein occlusion. The Central Vein Occlusion Study Group. *Arch Ophthalmol*. 1997;115(4):486–491.
20. Yang J, Zhang B, Wang E, Xia S, Chen Y. Ultra-wide field swept-source optical coherence tomography angiography in patients with diabetes without clinically detectable retinopathy. *BMC Ophthalmol*. 2021;21(1):192.
21. Shahlaee A, Samara WA, Hsu J, et al. In vivo assessment of macular vascular density in healthy human eyes using optical coherence tomography angiography. *Am J Ophthalmol*. 2016;165:39–46.
22. Chu Z, Lin J, Gao C, et al. Quantitative assessment of the retinal microvasculature using optical coherence tomography angiography. *J Biomed Opt*. 2016;21(6):66008.
23. Agrawal R, Chhablani J, Tan KA, Shah S, Sarvaiya C, Banker A. Choroidal vascularity index in central serous chorioretinopathy. *Retina*. 2016;36(9):1646–1651.
24. Tiew S, Lim C, Sivagnanasithiyar T. Using an excel spreadsheet to convert Snellen visual acuity to LogMAR visual acuity. *Eye (Lond)*. 2020;34(11):2148–2149.
25. Carpineto P, Mastropasqua R, Marchini G, Toto L, Di Nicola M, Di Antonio L. Reproducibility and repeatability of foveal avascular zone measurements in healthy subjects by optical coherence tomography angiography. *Br J Ophthalmol*. 2016;100(5):671–676.
26. Wons J, Pfau M, Wirth MA, Freiberg FJ, Becker MD, Michels S. Optical coherence tomography angiography of the foveal avascular zone in retinal vein occlusion. *Ophthalmologica*. 2016;235(4):195–202.
27. Adhi M, Filho MA, Louzada RN, et al. Retinal capillary network and foveal avascular zone in eyes with vein occlusion and fellow eyes analyzed with optical coherence tomography angiography. *Invest Ophthalmol Vis Sci*. 2016;57(9):486–494.
28. Suzuki N, Hirano Y, Tomiyasu T, et al. Retinal hemodynamics seen on optical coherence tomography angiography before and after treatment of retinal vein occlusion. *Invest Ophthalmol Vis Sci*. 2016;57(13):5681–5687.
29. Deng Y, Zhong QW, Zhang AQ, et al. Microvascular changes after conbercept therapy in central retinal vein occlusion analyzed by optical coherence tomography angiography. *Int J Ophthalmol*. 2019;12(5):802–808.
30. Çalışkan NE, Doğan M, Çalışkan A, Gobeka HH, Ay İE. Optical coherence tomography angiography evaluation of retinal and optic disc microvascular morphological characteristics in retinal vein occlusion. *Photodiagnosis Photodyn Ther*. 2022;41:103244.
31. Coscas F, Glacet-Bernard A, Miere A, et al. Optical coherence tomography angiography in retinal vein occlusion: evaluation of superficial and deep capillary plexa. *Am J Ophthalmol*. 2016;161:160–171.
32. Wakabayashi T, Sato T, Hara-Ueno C, et al. Retinal microvasculature and visual acuity in eyes with branch retinal vein occlusion: imaging analysis by optical coherence tomography angiography. *Invest Ophthalmol Vis Sci*. 2017;58(4):2087–2094.
33. Samara WA, Shahlaee A, Sridhar J, Khan MA, Ho AC, Hsu J. Quantitative optical coherence tomography angiography features and visual function in eyes with branch retinal vein occlusion. *Am J Ophthalmol*. 2016;166:76–83.
34. Freund KB, Sarraf D, Leong BCS, Garrity ST, Vupparaboina KK, Dansingani KK. Association of optical coherence tomography angiography of collaterals in retinal vein occlusion with major venous outflow through the deep vascular complex. *JAMA Ophthalmol*. 2018;136(11):1262–1270.
35. Tsuboi K, Sasajima H, Kamei M. Collateral vessels in branch retinal vein occlusion: anatomic and functional analyses by OCT angiography. *Ophthalmol Retina*. 2019;3(9):767–776.
36. Gallego-Pinazo R, Dolz-Marco R, Marín-Lambíes C, Díaz-Llopis M. Safety and efficacy of ranibizumab in macular edema following retinal vein occlusion. *Ophthalmol Eye Dis*. 2012;4:15–21.
37. Tang F, Xu F, Zhong H, et al. Comparison of subfoveal choroidal thickness in eyes with CRVO and BRVO. *BMC Ophthalmol*. 2019;19(1):133.
38. Chen L, Yuan M, Sun L, Chen Y. Choroidal thickening in retinal vein occlusion patients with serous retinal detachment. *Graefes Arch Clin Exp Ophthalmol*. 2021;259(4):883–889.
39. Tsuiki E, Suzuma K, Ueki R, Maekawa Y, Kitaoka T. Enhanced depth imaging optical coherence tomography of the choroid in central retinal vein occlusion. *Am J Ophthalmol*. 2013;156(3):543–547.
40. Lee EK, Han JM, Hyon JY, Yu HG. Changes in choroidal thickness after intravitreal dexamethasone implant injection in retinal vein occlusion. *Br J Ophthalmol*. 2015;99(11):1543–1549.
41. Wei WB, Xu L, Jonas JB, et al. Subfoveal choroidal thickness: the Beijing Eye Study. *Ophthalmology*. 2013;120(1):175–180.
42. Mastropasqua R, Toto L, Di Antonio L, et al. Optical coherence tomography angiography microvascular findings in macular edema due to central and branch retinal vein occlusions. *Sci Rep*. 2017;7:40763.
43. Wang Q, Chan SY, Yan Y, et al. Optical coherence tomography angiography in retinal vein occlusions. *Graefes Arch Clin Exp Ophthalmol*. 2018;256(9):1615–1622.
44. Costanzo E, Parravano M, Gilardi M, et al. Microvascular retinal and choroidal changes in retinal vein occlusion analyzed by two different optical coherence tomography angiography devices. *Ophthalmologica*. 2019;242(1):8–15.
45. Alis A, Guler Alis M. The effect of branch retinal vein occlusion on the vascular structure of the choroid. *Photodiagnosis Photodyn Ther*. 2022;37:102687.
46. Noma H, Funatsu H, Yamasaki M, et al. Pathogenesis of macular edema with branch retinal vein occlusion and intraocular levels of vascular endothelial growth factor and interleukin-6. *Am J Ophthalmol*. 2005;140(2):256–261.
47. Julien S, Biesemeier A, Taubitz T, Schraermeyer U. Different effects of intravitreally injected ranibizumab and aflibercept on retinal and choroidal tissues of monkey eyes. *Br J Ophthalmol*. 2014;98(6):813–825.
48. Mitamura Y, Enkhmaa T, Sano H, et al. Changes in choroidal structure following intravitreal aflibercept therapy for retinal vein occlusion. *Br J Ophthalmol*. 2021;105(5):704–710.
49. Kinoshita T, Mitamura Y, Mori T, et al. Changes in choroidal structures in eyes with chronic central serous chorioretinopathy after half-dose photodynamic therapy. *PLoS One*. 2016;11(9):e0163104.
50. Kase S, Endo H, Takahashi M, et al. Alteration of choroidal vascular structure in diabetic macular edema. *Graefes Arch Clin Exp Ophthalmol*. 2020;258(5):971–977.

Investigative Ophthalmology & Visual Science

51. Silva PS, Cavallerano JD, Haddad NM, et al. Peripheral lesions identified on ultrawide field imaging predict increased risk of diabetic retinopathy progression over 4 years. *Ophthalmology*. 2015;122(5):949–956.
52. Zhuang X, Chen R, Liang A, et al. Multimodal imaging analysis for the impact of retinal peripheral lesions on central neurovascular structure and retinal function in type 2 diabetes with diabetic retinopathy. *Br J Ophthalmol*. 2023;107(10):1496–1501.
53. Spaide RF, Fujimoto JG, Waheed NK, Sadda SR, Staurenghi G. Optical coherence tomography angiography. *Prog Retin Eye Res*. 2018;64:1–55.

Investigative Ophthalmology & Visual Science